

Effect of Multiple Cycles of Gelatinization and Fermentation in Chinese Strong-Flavor Baijiu on Sorghum Starch

Xuyan Zong

Sichuan University of Science and Engineering

Lei Wen

Sichuan University of Science and Engineering

Tingting Mou

Sichuan University of Science and Engineering

Yanting Wang

Beijing Forestry University

Li Li (✉ kokonice@139.com)

Sichuan University of Science and Engineering

Research Article

Keywords: Strong-flavor Baijiu, Gelatinization, Fermentation, Sorghum starch, Physicochemical property

Posted Date: May 18th, 2022

DOI: <https://doi.org/10.21203/rs.3.rs-1638260/v1>

License: © ⓘ This work is licensed under a Creative Commons Attribution 4.0 International License.

[Read Full License](#)

Abstract

The property changes of sorghum starch during multiple cycles of gelatinization fermentation were studied. This study simulated strong-flavor Baijiu's gelatinization and fermentation process (The sorghum as raw material, the distillers' grains as control). The results showed that the starch content of the same batch of sorghum after five cycles of gelatinization and fermentation was 9.98% (Cannot continue to be used for fermentation), and about 60% of the starch was consumed in the first three cycles of gelatinization and fermentation. The gel properties of sorghum starch gradually decreased during fermentation but slightly increased after gelatinization. After five cycles of gelatinization and fermentation, the sorghum starch has a uniform size and thin and small fragment structure. At the same time, sorghum starch does not form new groups. The recrystallization of starch caused by multiple cycles of gelatinization and fermentation increased the onset gelatinization temperature (from 61.6 to 114.4 °C), peak gelatinization temperature (from 78.5 to 139.5 °C), and gelatinization enthalpy (from 7.980 to 17.121 J/g) of sorghum starch. The crystalline structure of sorghum starch changed from the initial type A to type A+V, type A+B+V, and finally to type B.

Introduction

Strong-flavor Baijiu is produced by solid-state fermentation using sorghum and other grains. Sorghum contains about 70% of starch, and microorganisms can use this starch in Baijiu production. Sorghum contains moderate protein and low content of fat, resulting in the sorghum becoming a superior raw material for producing strong-flavor Baijiu (Appiah. et al., 2019; Qian et al., 2021). In Baijiu production, the utilization rate of starch is directly related to the liquor yield (Wang et al., 2020). However, the efficiency of fermentation is limited by the production efficiency of solid-state fermentation and the traditional Baijiu brewing technology, resulting in some starch from raw materials that can not be consumed by microorganisms and be discarded with distillers' grains (DGS, byproducts of Baijiu production), and affected the economic benefits, quality, and yield of Baijiu production (Li et al., 2021; Zhi et al., 2017).

The starch of raw materials undergoes multiple cycles of gelatinization and low-temperature fermentation because of the technology of strong-flavor Baijiu production. The essence of starch gelatinization is that the hydrogen bond between starch molecules is destroyed under the action of heat and water to form a hydrophilic colloidal solution, and starch gradually varies from semi-crystalline to an amorphous structure. Starch gradually changes from a disordered and high-energy state to an ordered and low-energy state under the action of molecular potential energy in the fermentation process (Fayin et al., 2019; Schirmer et al., 2014). Previous reports showed that gelatinization and fermentation affected the gel properties, crystalline structure, and granule morphology of sorghum starch (Elkhalifa, Schiffler, & Bernhardt, 2005; Sun, Han, Wang, & Xiong, 2014). However, the effect of multiple cycles of gelatinization and fermentation unique to Baijiu production on the properties of sorghum starch is unknown.

The production process of strong-flavor Baijiu was simulated to study the effect of multiple gelatinization and fermentation on sorghum starch in strong-flavor Baijiu. The changes of sorghum starch in multiple

gelatinization and fermentation were studied by gel analysis, scanning electron microscopy (SEM), X-ray diffraction (XRD), differential scanning calorimetry (DSC), and Fourier transform infrared reflection (FTIR). Meanwhile, the characteristics and reasons of sorghum starch in multiple gelatinization and fermentation were analyzed in combination with Baijiu production technology. This study is of guiding significance for methods to improve starch's utilization efficiency and transformation efficiency in Baijiu production.

Materials And Methods

Materials

Sorghum and *Daqu* (market procurement); Total Starch Assay Kit (Shanghai *Huicheng* Biotechnology Co., Ltd. Shanghai, China); Amylose Assay Kit (Hefei *Laier* Biotechnology Co., Ltd. Anhui, China); All reagents and chemicals used were of analytical grade (Chengdu Kelong Chemical Reagent Factory, Sichuan, China).

Technological process of gelatinization

The technological process of gelatinization is shown in **Fig S1**. Sorghum was used as raw material for multiple cycles of gelatinization and fermentation. Samples were taken after each gelatinization and the first, fourth, and seventh day of each fermentation cycle, and Baijiu distillers' grains were used as controls. All samples were pretreated by wet screening, water washing, and centrifugation to remove rice hulls and water-soluble substances.

Starch separation

The starch separation according to the method of Rittenauer et al. with modifications (Rittenauer et al., 2016). The samples of *Zaopei* with different gelatinization and fermentation cycles were taken, mixed with an appropriate amount of distilled water, screened with 20 mesh, then centrifuged three times (5000r / min, 5min), and freeze-dried for 24h. The dried sample was put into an extraction flask with 5.0g and extracted with 2/3 of petroleum ether for 2 h. After that, the sample was taken out and placed for several hours until the petroleum ether volatilizes completely. Added ethanol (90%) (solid-liquid ratio: 1g: 10ml) to the above samples and stirred evenly at room temperature, and centrifuged three times (5000r / min, 10min) after keeping in water at 50 °C for 2h, and collected the supernatant. Ethanol (90%) (the ratio of material to liquid is 1g:10ml) was added to the sediment again. After a water bath for 2h (5 °C), centrifuging three times (5000r / min, 10min), the supernatant was combined, and the starch content was measured. The two sediments were collected and then freeze-dried.

Starch content

The total starch content of sorghum was determined by the Total Starch Assay Kit. Weighed 100mg of sample (35 mesh sieve) and mixed with 0.2ml of ethanol solution (80%), immediately added 2ml of DMSO (dimethyl sulfoxide), boiling water bath for 5min (shaking the tube), then put the tube in 50°C

water bath and added 0.1ml of amyloglucosidase (3300U/ml) and kept for 30min. The above solution was diluted to 100ml, part of the solution was centrifuged (3000rpm, 10min), and the supernatant was taken. The 0.1ml supernatant was mixed with 3ml GOPOD (including glucose oxidase > 12000U, peroxidase > 650U, 4-amino antipyrine 80mg) solution and then water bath (50°C) for 20min, and the absorbance of the sample was measured at 510nm. The glucose control included 0.1mL glucose standard solution (1mg/mL), 3.0mL GOPOD solution. The blank reagent control included 0.1mL distilled water and 3.0mL GOPOD solution. The total starch content was calculated according to the following formula.

$$Totalstarch(\%) = \Delta A \times \frac{F}{W} \times FV \times 0.9 \#(1)$$

Where: ΔA = Absorbance of sample

$F = 100 (\mu\text{g of D-glucose}) / \text{Absorbance for } 100 \mu\text{g of glucose}$

$FV = \text{Total volume}$

$W = \text{Mass of sample}$

The amylose content of sorghum was determined by Amylose Assay Kit. Weighed 0.1 mg of sample and mixed with 1 ml of DMSO (to ensure no lumps), and boiling water bath for 15 min. After cooling to room temperature, added 6ml of ethanol (95%), placed for 15 min and then centrifuged (2000rpm, 5min), collected the sediment and placed until the ethanol volatilizes. Then added 2ml of DMSO to the sediment. After boiling water bath (15min), 4ml of ConA solution was added immediately and then diluted to 25ml with ConA. The 1ml of the above sample solution was mixed with 3ml of sodium acetate solution (100mM,pH4.5), After boiling water bath (5min) and then held in a water bath at 40°C for 5min, and 1ml of a mixture of starch transglucosidase and α -amylase was added and reacted for 30min and then centrifuged (2000rpm, 5min). The absorbance of samples and glucose control was measured at 510nm after taking 1ml of supernatant and mixed with 4ml of GOPOD reagent at 40°C for 20min. The amylose content was calculated according to the following formula.

$$Amylose(\%) = \frac{2 \times \Delta A_1}{W \times \Delta A_2} \#(2)$$

Where: ΔA_1 = Absorbance of sample

ΔA_2 = Absorbance of standard glucose solution

$W = \text{Mass of sample}$

Starch gel properties

Light transmittance

The light transmittance was determined using a method described by Faiza Shaikh et al. (Shaikh et al., 2019) with modifications. The 0.50 g starch (dry basis) was prepared into starch milk (1%) with distilled water. The starch milk was cold to room temperature after a boiling water bath. Starch milk was poured into a 1 cm cuvette and determined light transmittance (620 nm, distilled water as control) with an ultraviolet spectrophotometer (UV2400, Beijing Purkinje General Instrument Co., Ltd., China).

Water-holding capacity

According to a method of Abhari et al. (Abhari et al., 2017) with modifications. The 1.0 g starch (dry basis) and 15 mL distilled water were put in a centrifuge tube and stirred evenly. The starch solution was centrifuged (3000 x g) (Allegra 64R, Beckman Coulter Co., Ltd., USA) for 10 min after shaking at room temperature for 1 h. The centrifuge tube was tilted slightly after discarding the supernatant. The droplets on the inner and outer tube walls and supernatant were absorbed after standing for 10 min. The water holding capacity was the mass of water absorbed per gram of sample.

$$\text{Waterholdingcapacity}(g/g) = \frac{m_2 - m_1 - m}{m} \#(3)$$

Where: m = Mass of sample (dry basis)

m_1 = Mass of centrifuge tube (with lid)

m_2 = Sum of m_1 and mass of sediment

Freeze-thaw stability

The freeze-thaw stability of starch was determined using the Zhang et al. (Zhang et al., 2019) method with modifications. The 3.0 g starch sample (dry basis) and the distilled water were prepared into starch solution (6%). The appropriate amount of starch solution was transferred into a centrifuge tube (50 mL) and a boiling water bath for 30 min. The starch solution was placed in the refrigerator (-18°C) for 12 hrs after cooling to room temperature. The frozen starch solution was thawed for 6 hrs at room temperature and centrifuged (3000 x g) for 20 min. The centrifuge tube was weighed after discarding the supernatant, and starch samples were freeze-thawed three times. The syneresis rate expresses the freeze-thaw stability.

$$\text{syneresisrate}(\%) = \frac{(M_1 - M_2) \times 100}{(M_1 - M_0)} \#(4)$$

Where: M_0 = Mass of the centrifuge tube

M_1 = Mass of the centrifuge tube and starch solution before freezing

M_2 = Mass of centrifuge tube and sediments after discarding the supernatant

Solubility and swelling power

According to a method of Farrag et al.(Farrag et al., 2018) with modifications. The 1.0 g starch sample (dry basis) and the distilled water were prepared into starch solution (2%). The starch solution (25 mL) was transferred into the two centrifuge tubes (50 mL) and put into water bath pots (30°C and 70°C) for 30 min (stirring continuously during the water bath). The starch solution was centrifuged (5000 x g) for 10 min after cooling to room temperature. The supernatant was poured into two glass dishes, respectively, and most of the water was evaporated in a 90°C water bath. The two glass dishes were dried to constant weight in the electric thermostatic drying oven (105°C).

$$Solubility(\%) = \frac{A \times 100}{M} \#(5)$$

$$Swellingpower(\%) = \frac{P \times 100}{M \times (1 - S)} \#(6)$$

Where: A = mass of starch on the glass dish

P = mass of sediments

M = mass of the starch sample (dry basis)

S = Solubility

Sorghum starch structure

Scanning electron microscope (SEM)

Scanning electron micrographs were taken by a VEGA 3SBU Scanning Electron Microscope (VEGA 3SBU, TESCAN Ltd., The Czech Republic) at an accelerating voltage of 3 kV. The dried starch samples were evenly applied on the double-sided adhesive tape and coated with gold for 120 s.

Fourier transform infrared reflection (FTIR)

The 3 mg of starch sample dried to constant weight, and 300 mg of potassium bromide powder were mixed and ground for 10 min, and then passed 100 mesh sieve. The mixed powder was pressed into tablets and used for FT-IR measurement (Nicolet6700, Thermofisher Ltd., USA). The potassium bromide was used as blank control. The spectra were recorded from 400 to 4000 cm^{-1} , and the resolution is 4 cm^{-1} . Each sample was determined three times.

X-ray diffraction

XRD patterns of starch were prepared using an X-ray diffractometer (D2PHASER, Bruker AXS Ltd., Germany). Measurements were obtained at 40 kV of tube voltage with a scanning rate of 0.02°/s and a diffraction angle range of 5° to 90°. The relative crystallinity was calculated using peak fitting software.

Differential scanning calorimetry (DSC)

The 3 mg sorghum starch and 10 μ L ultrapure water were mixed and sealed and then placed at room temperature for 3 hrs and used for DSC measurement (DSC200F3, Netzsch Ltd., Germany). The sealed, empty aluminum box is the blank control. Measurements were obtained with a scanning rate of 10°C/min and a scanning range of 30°C to 150°C. The parameters in the gelatinization process of sorghum starch were analyzed and compared, including onset gelatinization temperatures (T_0), peak gelatinization temperatures (T_p), conclusion gelatinization temperatures (T_c), and gelatinization enthalpy (ΔH).

Statistical analysis

All the experiments were performed at least in triplicate. One-way analysis of variance (ANOVA) by SPSS 24.0 (SPSS Inc., Chicago) was used to establish differences among data. Data of experiments were analyzed by Origin 2021 (Origin Lab Company, USA).

Results And Discussions

Composition of sorghum starch

As shown in Fig. 1, the total starch content shows a downward trend, and the amylose content shows a significant increase at first and then a slight decrease. Starch molecules are degraded by the enzymes and organic acids produced during multiple cycles of gelatinization and fermentation, resulting in a decrease in total starch content. In the fermentation process, the linear amylose molecular chain is produced by the chain breaking, and debranching of amylopectin, and the consumption of amylose is less than that of amylopectin, increasing amylose content. The amylose content was about 60% of the total starch content in the fifth cycle of gelatinization and fermentation. More amylose is degraded by enzymes and acids than amylopectin (Xu, Waters, Blanchard, & Tan, 2021), resulting in a slight decrease in amylose content. In the first to the third cycle of gelatinization and fermentation, the total starch content decreased the most, which may be because the starch and nutrients are abundant in the first three cycles of gelatinization and fermentation, and most of the starch is consumed and utilized by microorganisms like *Rhizopus*, *Saccharomyces cerevisiae*, *Acetobacter*, *Lactobacillus*, etc. In addition, the total starch content decreased slightly and gradually stabilized after the fourth cycle of gelatinization and fermentation, indicating that the starch that microorganisms can use is almost consumed at this time.

The total starch content on the first day of fermentation decreased the most compared with the fourth and seventh days of fermentation, which may be because the high starch content improves the utilization efficiency of microorganisms for starch in the early stage of fermentation (for their growth or converting starch into other substances). The study showed that the acidity and moisture in the *Zaopei* gradually increase with fermentation days, and excessive acidity and byproduct inhibit the action of enzymes and microorganisms, resulting in the consumption rate of starch decreased (Yan et al., 2011). The growth of dominant fermentation strains was poor due to too little starch content and the breeding of miscellaneous bacteria when the sixth cycle of gelatinization and fermentation was tried. Therefore, gelatinization and fermentation are only carried out until the fifth cycle.

Sorghum starch gel properties

Solubility and swelling power

The solubility of starch generally shows a downward trend, and the swelling power first decreases and then increases slightly with the increase of gelatinization and fermentation cycles (Fig. 2a, b), which may be because enzymes and acids hydrolyze the amylopectin. The hydrogen bond between amylose molecules forms a double helix structure, and the amylose forms a complex with substances such as lipids, resulting in the decrease of hydration, swelling power, and solubility of starch. The amylose began to be degraded in the fifth cycle of gelatinization and fermentation, resulting in a slight increase in the swelling power of starch. This result is consistent with the previously reported conclusion that the solubility of starch is positively correlated with the content of amylopectin, and the swelling power is negatively correlated with the content of amylose (Cai et al., 2015).

The solubility and swelling power of sorghum starch at 70°C are significantly higher than that at 30°C because the hydrogen bond is easier to break at high temperatures, and the crystalline structure of starch is more damaged than sorghum starch at 30°C. The looseness of the crystalline region strengthens the water-binding capacity of starch (Li et al., 2015), resulting in an increase in the solubility and swelling power. This result is also why the swelling power of fermented sorghum starch increases after gelatinization.

Light transmittance

The light transmittance of starch decreases gradually with the fermentation process and increases slightly after each cycle of gelatinization (Fig. 2c). The decrease in light transmittance may be due to the stable structure of starch molecules with starch molecules and other substances during fermentation and the birefringence phenomenon (Xu et al., 2021). The slight increase of light transmittance is that each cycle of gelatinization has great damage to the stable structure formed by starch molecules and other substances. The light transmittance of starch decreased significantly in the first three cycles of gelatinization and fermentation (the light transmittance decreased from 12.98–5.10%). The significant increase of amylose at this stage and the intense recrystallization and retrogradation of starch may decrease starch light transmittance.

Freeze-thaw stability and water-holding capacity

The water-holding capacity of starch decreases during the first four fermentation cycles and increases slightly in the fifth cycle of fermentation (Fig. 2d). The decrease in the water holding capacity of sorghum starch during the first four fermentation cycles may be due to the structure of the starch is damaged after gelatinization, which loosens the microcrystal strand region of the starch and dissolves the amylose from the dissolved starch granules. During low-temperature fermentation, the amylopectin in the amorphous region is hydrolyzed by enzymes, and the amylose that is easier to rearrange increased, forming a double helix structure. In addition, the recrystallization of starch forms a more compact structure, reducing the

binding sites between starch granules and water molecules, resulting in a decrease in water holding capacity (Zhang et al., 2019). Microorganisms mainly used amylose in the fifth cycle of fermentation and produced more binding sites of the water molecules, resulting in a slight increase in water holding capacity. Microorganisms mainly use amylose in the fifth cycle of fermentation and produced more binding sites of the water molecules, resulting in a slight increase in water-holding capacity. The water-holding capacity of starch increases slightly after each gelatinization because gelatinization destroys the crystalline structure of starch, and exposes more hydrophilic groups, which is conducive to the combination of starch molecules and water molecules (Xu et al., 2021).

The freeze-thaw stability of starch decreased with the progress of multiple cycles of gelatinization and fermentation (Fig. 2e). The freeze-thaw stability of starch is slightly improved after gelatinization because gelatinization improves the water-binding capacity of starch (Li et al., 2015) and reduces the syneresis rate of starch. In addition, the increase in freeze-thaw cycles also increases the syneresis rate of starch.

Structure of sorghum starch

Granule morphology

It can be seen from Fig. 3 that most of the natural sorghum starch granules are smooth, and quasi-circular, and a few are irregular polygons with small granule sizes. After gelatinization and fermentation, the sorghum starch granules showed irregular blocks with rough surfaces and larger granule sizes. Starch granules lost their original morphology after five cycles of gelatinization and fermentation. After the first three cycles of gelatinization fermentation, the pores on the surface of starch granules increased, and the pore size gradually became more noticeable. This result is because amylose molecules are rearranged to form blocky granules with larger granule sizes. In addition, starch molecules are incompletely hydrolyzed by microorganisms and acids, resulting in many deep pores on the surface of starch.

The size of starch granules was gradually uniform in the fourth cycle of gelatinization and fermentation, from blocky to small and thin fragments. However, there were still little blocky starch granules, indicating that some starch has not been hydrolyzed by enzyme, and this part of starch has a specific resistance to the enzyme system in solid-state fermentation. This result may be due to the recrystallization of amylose or the complex formed by amylose and lipids, which increases the enzymatic hydrolysis resistance of starch (Chang et al., 2021; Kang et al., 2021). The morphology of sorghum starch granules was similar to that in the distillers' grains after the fifth cycle of gelatinization and fermentation. They were small, thin, and uniform fragments, and there were also little blocky starch granules.

Fourier transform infrared reflection

After multiple cycles of gelatinization and fermentation, the characteristic absorption peak of sorghum starch only varies in intensity without significant displacement and no new absorption peak (Fig. 4a), indicating that multiple cycles of gelatinization and fermentation did not affect the chemical groups of sorghum starch. The characteristic absorption peaks at 856 cm^{-1} , 766 cm^{-1} , and 578 cm^{-1} correspond

to the stretching and vibrations of the glucose unit (Flores et al., 2012). The characteristic absorption peak of the glucose unit was lost in the starch from distillers' grains and the starch from the fourth and fifth cycles of gelatinization and fermentation, indicating the glucose content in sorghum starch decreased at this stage. This result is because sorghum starch is heavily used and transformed by microorganisms in the first three cycles of gelatinization and fermentation. The starch content was low in the last two cycles of gelatinization and fermentation, resulting in little glucose production. In addition, some starch with resistance to enzymatic hydrolysis also inhibits glucose production.

Differential scanning calorimetry

It can be seen from Fig. 4b and Table 1 that the onset gelatinization temperatures (T_0) and peak gelatinization temperatures (T_p) of sorghum starch increase with the increase of gelatinization and fermentation cycles, which may be because sorghum starch granules gather internally during fermentation, and the structures of the amorphous region and metastable region become more stable, resulting in the increased difficulty of gelatinization. The increase of gelatinization enthalpy (ΔH) is caused by the more and more stable crystalline region in starch granules during fermentation, which is consistent with the conclusion by Samson et al. (Oyeyinka et al., 2020) that fermentation improves the onset gelatinization temperatures, peak gelatinization temperatures, and conclusion gelatinization temperatures (T_c) of starch.

Table 1
Gelatinization results of sorghum starch and distillers' grains

Starch samples	$T_0/^\circ\text{C}$	$T_p/^\circ\text{C}$	$T_c/^\circ\text{C}$	$\Delta H/(\text{J/g})$
Raw sorghum	61.6	78.5	91.8	7.980
Gelatinization and fermentation- cycle 1	103.1	132.8	142.6	11.931
Gelatinization and fermentation- cycle 2	105.2	134.0	139.7	13.740
Gelatinization and fermentation- cycle 3	108.6	137.3	146.0	14.739
Gelatinization and fermentation- cycle 4	109.1	135.4	139.7	15.567
Gelatinization and fermentation- cycle 5	114.4	139.5	144.8	17.121
DGS	112.0	139.4	147.0	16.811

X-ray diffraction

The crystalline structure of sorghum starch varies from type A to type A + V and type A + B + V, and finally to type B (Fig. 4c, Table 2) after multiple cycles of gelatinization and fermentation. The characteristic diffraction peaks of 12.9° and 19.8° appeared in sorghum starch after the first cycle of gelatinization fermentation, and the corresponding sorghum starch crystalline structure varied from type A to type A + V.

The appearance of type V crystalline structure indicates the formation of a starch complex (Chen et al., 2019). The characteristic diffraction peak of 16.9° appeared in sorghum starch after the fourth cycle of gelatinization and fermentation, indicating that the type B structure appeared, and its formation is caused by starch retrogradation (Chen et al., 2019).

Table 2
XRD results of sorghum starch and distillers' grains

Starch samples	Diffraction peak position(°)	Crystalline type	Crystallinity(%)
Raw sorghum	15.17-18.23	A	30
Gelatinization and fermentation-cycle 1	12.9-14.8-16.7-19.8	A + V	27.28
Gelatinization and fermentation-cycle 2	13.1-16.8-18.5-19.5	A + V	23.08
Gelatinization and fermentation-cycle 3	13.0-15.0-17.6-19.6	A + V	20.32
Gelatinization and fermentation-cycle 4	12.9-16.9-19.7-22.2	A + B + V	16.46
Gelatinization and fermentation-cycle 5	17.8-26.6	B	9.39
DGS	16.9-21.8-26.6	B	11.01

The characteristic diffraction peaks of 26.6° and 17.8° appeared in sorghum starch after the fifth cycle of gelatinization fermentation, indicating that the type V structure disappeared, which may be because the microorganisms mainly consumed amylose during the fifth cycle of fermentation, resulting in the low content of the starch complex. The characteristic diffraction peak of 26.6° appeared in sorghum starch after the fifth cycle of gelatinization fermentation and DGS (the crystallinity is very close), indicating that the crystalline structure is close to the same. The relative crystallinity of sorghum starch decreased gradually after multiple cycles of gelatinization and fermentation (from 30.00–9.39%), which may be because the crystalline region of starch recrystallization is less than that of the original sorghum starch. Hence, the relative crystallinity of starch decreases in continuous recrystallization.

Conclusion

This study found that the starch content of the same batch of sorghum after five cycles of gelatinization and fermentation was 9.98%, which was no longer suitable for a new cycle of gelatinization and fermentation. The changes in sorghum starch properties in five cycles of gelatinization and fermentation were studied. The results showed that the gel properties of sorghum starch gradually decreased during fermentation, and slightly increased after gelatinization; Sorghum starch varies from smooth quasi-

circular granules to rough irregular block structures with noticeable pores in the process of five cycles of gelatinization and fermentation, and finally forms small and thin fragment structures with uniform size; Sorghum starch did not form new groups after five cycles of gelatinization and fermentation, but the characteristic absorption peak caused by the stretching and vibrations of the glucose unit disappeared at $1000\text{cm}^{-1} \sim 50\text{cm}^{-1}$ of the fingerprint region of starch, indicating that the amorphous region of starch was hydrolyzed first; The onset gelatinization temperature, peak gelatinization temperature, and gelatinization enthalpy of sorghum increased after five cycles of gelatinization and fermentation, and the crystalline structure of sorghum starch varied from the initial type A to type A + B + V, and finally to type B.

Declarations

Ethical Approval

(Not applicable)

Consent to Participate

(Not applicable)

Consent to Publish

(Not applicable)

Funding

This study was funded by the Sichuan Science and Technology Program: Research and Application of Key Technologies for Efficient Utilization of Starch in Strong-Flavor Baijiu Production [2018JZ0039].

Competing Interests

The authors declare they have no financial interests

Availability of data and materials

The datasets generated during and analyzed during the current study are available from the corresponding author on reasonable request.

Authors Contributions

Conceptualization: [Xuyan Zong] [Lei Wen] [Tingting Mou] [Li Li]; Data curation: [Xuyan Zong] [Lei Wen] [Tingting Mou]; Formal analysis: [Xuyan Zong] [Lei Wen] [Tingting Mou] [Li Li]; Funding acquisition: [Xuyan Zong] [Li Li]; Investigation: [Xuyan Zong] [Lei Wen] [Tingting Mou]; Project administration: [Xuyan Zong] [Li Li]; Resources: [Xuyan Zong] [Li Li]; Supervision: [Xuyan Zong] [Li Li]; Visualization: [Xuyan Zong] [Lei Wen] [Yanting Wang] [Li Li]; Writing-original draft: [Xuyan Zong] [Lei Wen] [Yanting Wang]; Writing-review&editing: [Xuyan Zong] [Li Li].

References

1. Abhari, N., Madadlou, A., Dini, A., & Hosseini Naveh, O. (2017). Textural and cargo release attributes of trisodium citrate cross-linked starch hydrogel. *Food Chemistry*, *214*, 16–24. doi:10.1016/j.foodchem.2016.07.042
2. Appiah-Nkansah, N. B., Li, J., Rooney, W., & Wang, D. (2019). A review of sweet sorghum as a viable renewable bioenergy crop and its techno-economic analysis. *Renewable Energy*, *143*, 1121–1132. doi:10.1016/j.renene.2019.05.066
3. Cai, J., Man, J., Huang, J., Liu, Q., Wei, W., & Wei, C. (2015). Relationship between structure and functional properties of normal rice starches with different amylose contents. *Carbohydr Polym*, *125*, 35–44. doi:10.1016/j.carbpol.2015.02.067
4. Chang, R., Jin, Z., Lu, H., Qiu, L., Sun, C., & Tian, Y. (2021). Type III Resistant Starch Prepared from Debranched Starch: Structural Changes under Simulated Saliva, Gastric, and Intestinal Conditions and the Impact on Short-Chain Fatty Acid Production. *Journal of Agricultural and Food Chemistry*, *69*(8), 2595–2602. doi:10.1021/acs.jafc.0c07664
5. Chen, L., Tian, Y., McClements, D. J., Huang, M., Zhu, B., Wang, L., Sun, B., Ma, R., Cai, C., & Jin, Z. (2019). A simple and green method for preparation of non-crystalline granular starch through controlled gelatinization. *Food Chemistry*, *274*, 268–273. doi:10.1016/j.foodchem.2018.09.006
6. Elkhalfifa, A., Schiffler, B., & Bernhardt, R. (2005). Effect of fermentation on the functional properties of sorghum flour. *Food Chemistry*, *92*(1), 1–5. doi:10.1016/j.foodchem.2004.05.058
7. Farrag, Y., Sabando, C., Rodriguez-Llamazares, S., Bouza, R., Rojas, C., & Barral, L. (2018). Preparation of donut-shaped starch microgranules by aqueous-alcoholic treatment. *Food Chemistry*, *246*, 1–5. doi:10.1016/j.foodchem.2017.10.147
8. Fayin, Xiao, Ya'nan, Liang, Yun, Zhou, Guohua, & Zhao. (2019). Spontaneous fermentation tunes the physicochemical properties of sweet potato starch by modifying the structure of starch molecules. *Carbohydrate polymers*. doi:10.1016/j.carbpol.2019.02.077
9. Flores-Morales, A., Jimenez-Estrada, M., & Mora-Escobedo, R. (2012). Determination of the structural changes by FT-IR, Raman, and CP/MAS (13)C NMR spectroscopy on retrograded starch of maize tortillas. *Carbohydr Polym*, *87*(1), 61–68. doi:10.1016/j.carbpol.2011.07.011
10. Kang, X., Sui, J., Qiu, H., Sun, C., Zhang, H., Cui, B., & Abd El-Aty, A. M. (2021). Effects of wheat protein on the formation and structural properties of starch-lipid complexes in real noodles incorporated with fatty acids of varying chain lengths. *Lwt*, *144*. doi:10.1016/j.lwt.2021.111271

11. Li, E., Yang, C., Wang, J., Sun, A., & Li, C. (2021). Leached starch content and molecular size during sorghum steaming for baijiu production is not determined by starch fine molecular structures. *International Journal of Biological Macromolecules*(22). doi:10.1016/j.ijbiomac.2021.06.031
12. Li, W., Tian, X., Liu, L., Wang, P., Wu, G., Zheng, J., Ouyang, S., Luo, Q., & Zhang, G. (2015). High pressure induced gelatinization of red adzuki bean starch and its effects on starch physicochemical and structural properties. *Food Hydrocolloids*, *45*, 132–139. doi:10.1016/j.foodhyd.2014.11.013
13. Oyeyinka, S. A., Adeloye, A. A., Olaomo, O. O., & Kayitesi, E. (2020). Effect of fermentation time on physicochemical properties of starch extracted from cassava root. *Food Bioscience*, *33*. doi:10.1016/j.fbio.2019.100485
14. Qian, W., Lu, Z. M., Chai, L. J., Zhang, X. J., Li, Q., Wang, S. T., Shen, C. H., Shi, J. S., & Xu, Z. H. (2021). Cooperation within the microbial consortia of fermented grains and pit mud drives organic acid synthesis in strong-flavor Baijiu production. *Food Research International*, *147*, 110449. doi:10.1016/j.foodres.2021.110449
15. Rittenauer, M., Kolesnik, L., Gastl, M., & Becker, T. (2016). From native malt to pure starch – Development and characterization of a purification procedure for modified starch. *Food Hydrocolloids*, *56*, 50–57. doi:10.1016/j.foodhyd.2015.11.025
16. Schirmer, M., Jekle, M., & Becker, T. (2014). Starch gelatinization and its complexity for analysis. *Starch - Stärke*. doi:10.1002/star.201400071
17. Shaikh, F., Ali, T. M., Mustafa, G., & Hasnain, A. (2019). Comparative study on effects of citric and lactic acid treatment on morphological, functional, resistant starch fraction and glycemic index of corn and sorghum starches. *Int J Biol Macromol*, *135*, 314–327. doi:10.1016/j.ijbiomac.2019.05.115
18. Sun, Q., Han, Z., Wang, L., & Xiong, L. (2014). Physicochemical differences between sorghum starch and sorghum flour modified by heat-moisture treatment. *Food Chemistry*, *145*, 756–764. doi:10.1016/j.foodchem.2013.08.129
19. Wang, B., Wu, Q., Xu, Y., & Sun, B. (2020). Synergistic Effect of Multi-Saccharifying Enzymes on Alcoholic Fermentation for Chinese Baijiu Production. *Applied and Environmental Microbiology*, *86*(8). doi:10.1128/AEM.00013-20
20. Xu, F., Zhang, L., Liu, W., Liu, Q., Wang, F., Zhang, H., Hu, H., & Blecker, C. (2021). Physicochemical and Structural Characterization of Potato Starch with Different Degrees of Gelatinization. *Foods*, *10*(5). doi:10.3390/foods10051104
21. Xu, X., Waters, D., Blanchard, C., & Tan, S. H. (2021). A study on Australian sorghum grain fermentation performance and the changes in Zaopei major composition during solid-state fermentation. *Journal of Cereal Science*, *98*. doi:10.1016/j.jcs.2021.103160
22. Yan, S., Wu, X., Bean, S. R., Pedersen, J. F., Tesso, T., Chen, Y. R., & Wang, D. (2011). Evaluation of Waxy Grain Sorghum for Ethanol Production. *Cereal Chemistry*, *88*(6). doi:10.1094/CCHEM-04-11-0056
23. Zhang, Y., Chen, C., Chen, Y., & Chen, Y. (2019). Effect of rice protein on the water mobility, water migration and microstructure of rice starch during retrogradation. *Food Hydrocolloids*, *91*, 136–142.

24. Zhang, Y., Li, G., Wu, Y., Yang, Z., & Ouyang, J. (2019). Influence of amylose on the pasting and gel texture properties of chestnut starch during thermal processing. *Food Chemistry*, 294, 378–383. doi:10.1016/j.foodchem.2019.05.070
25. Zhi, Y., Wu, Q., & Xu, Y. (2017). Production of surfactin from waste distillers' grains by co-culture fermentation of two *Bacillus amyloliquefaciens* strains. *Bioresource Technology*, 235, 96–103. doi:10.1016/j.biortech.2017.03.090

Figures

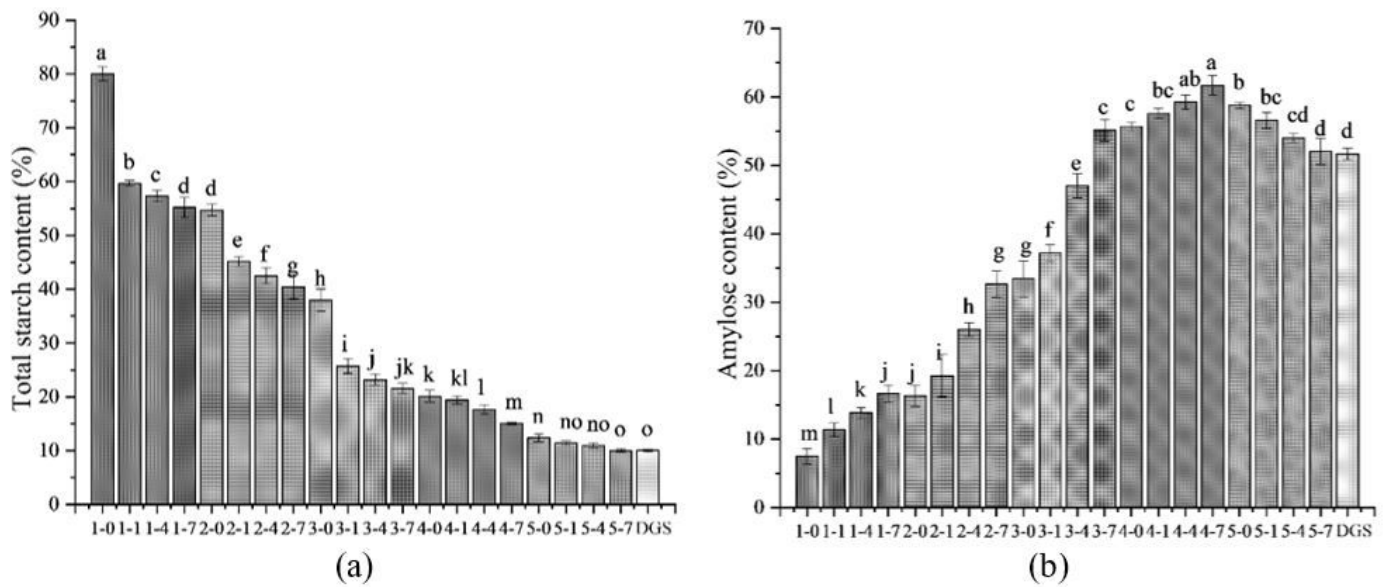


Figure 1

Starch content of each cycle of gelatinization and fermentation. (a) Total starch content (b) Amylose content. Different letters above the bars represent a significant difference between sorghum starch samples ($p < 0.05$)

Note: 1-0, 2-0, 3-0, 4-0, 5-0 represent sorghum starch samples after the first to fifth cycles of gelatinization, respectively; 1-1, 2-1, 3-1, 4-1, 5-1 represent sorghum starch samples on the first day of the first to fifth cycles of fermentation, respectively; 1-4, 2-4, 3-4, 4-4, 5-4 represent sorghum starch samples on the fourth day of the first to fifth cycles of fermentation, respectively; 1-7, 2-7, 3-7, 4-7, 5-7 represent sorghum starch samples on the seventh day of the first to fifth cycles of fermentation, respectively

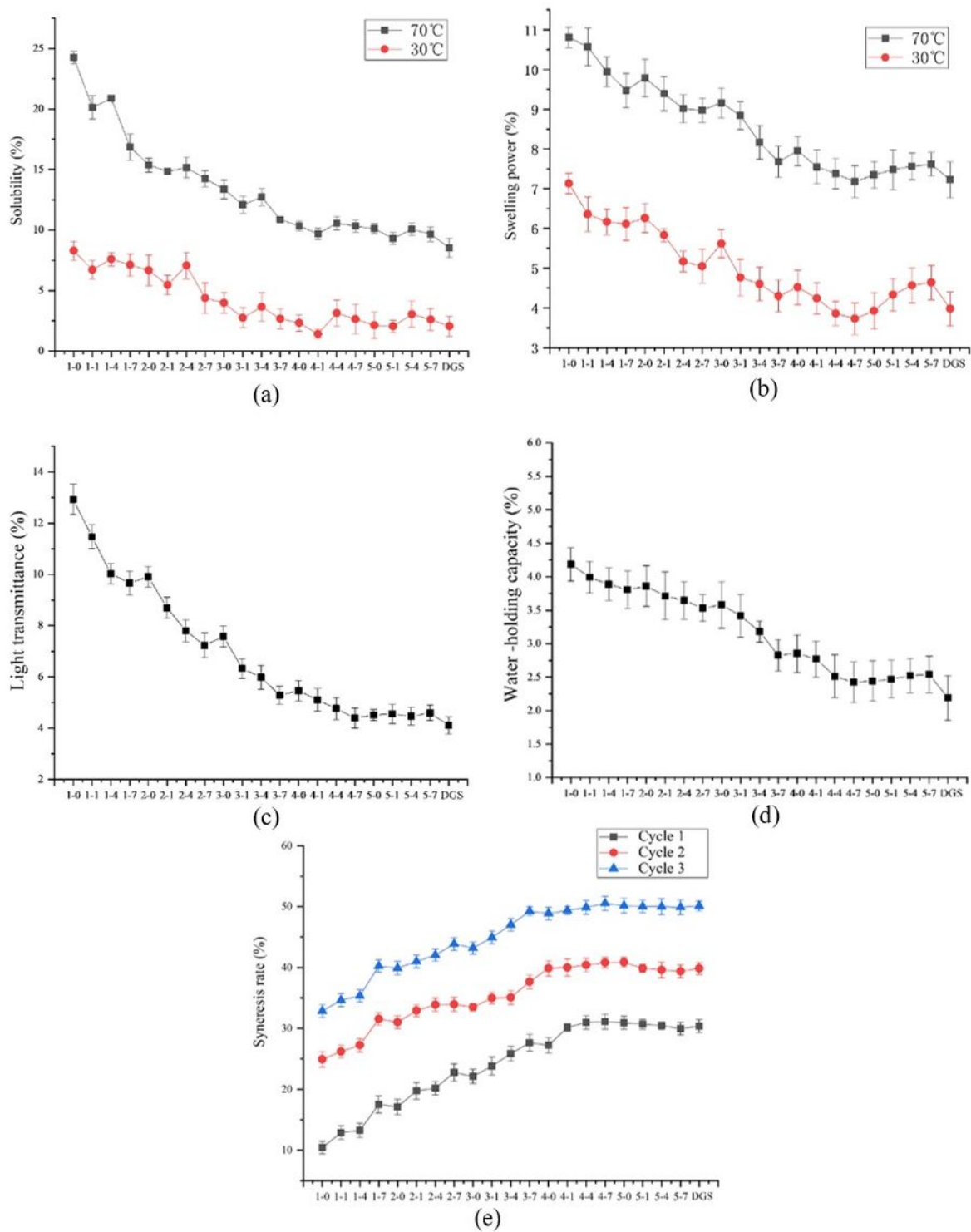


Figure 2

Gel properties of sorghum starch and distillers' grains starch. (a) Solubility (b) Swelling power (c) Light transmittance (d) Water-holding capacity (e) Freeze-thaw stability

Note: 1-0, 2-0, 3-0, 4-0, 5-0 represent sorghum starch samples after the first to fifth cycles of gelatinization, respectively; 1-1, 2-1, 3-1, 4-1, 5-1 represent sorghum starch samples on the first day of the first to fifth

cycles of fermentation, respectively; 1-4, 2-4, 3-4, 4-4, 5-4 represent sorghum starch samples on the fourth day of the first to fifth cycles of fermentation, respectively; 1-7, 2-7, 3-7, 4-7, 5-7 represent sorghum starch samples on the seventh day of the first to fifth cycles of fermentation, respectively

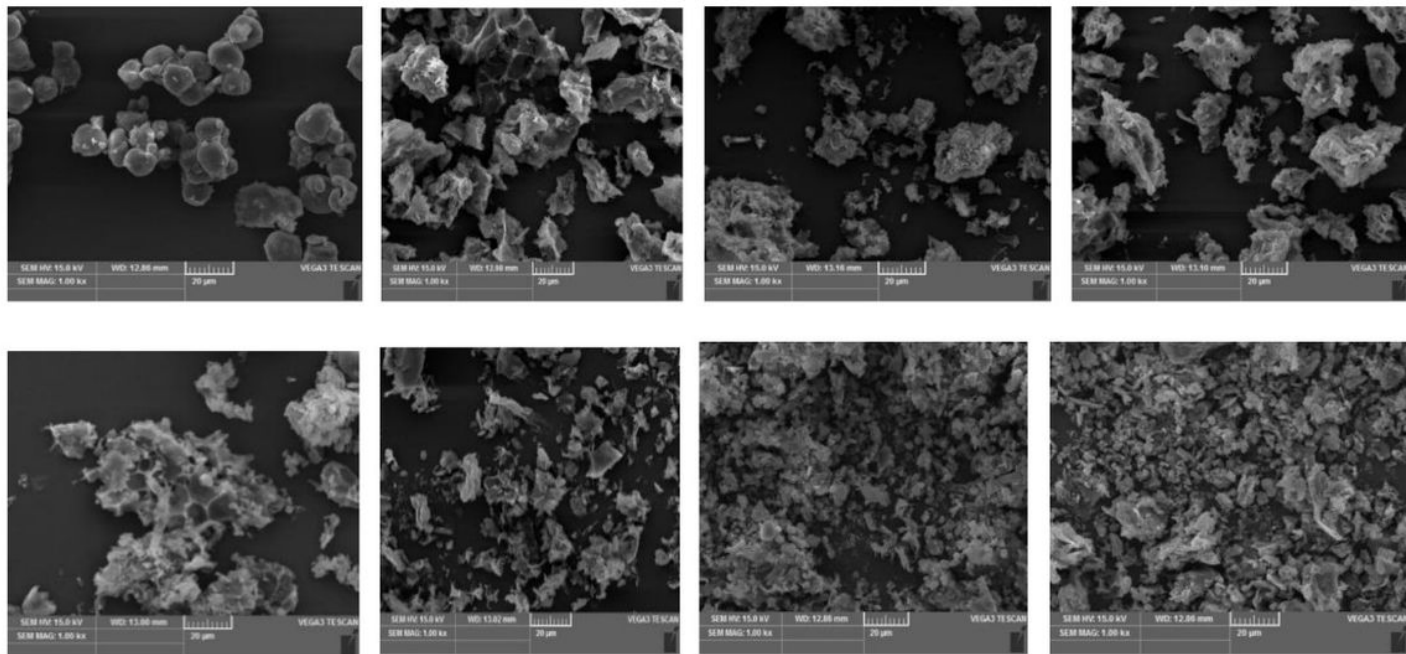


Figure 3

Granules morphology of sorghum starch and distillers' grains starch (x1000)

Note: The first row from left to right respectively represents the raw sorghum starch, the starch after the first cycle of gelatinization (unfermented), the starch after the first cycle of gelatinization (fermentation day 7), the starch after the second cycle of gelatinization (fermentation day 7). The second row from left to right respectively represents the starch after the third cycle of gelatinization (fermentation day 7), the starch after the fourth cycle of gelatinization (fermentation day 7), the starch after the fifth cycle of gelatinization (fermentation day 7), the distillers' grains starch

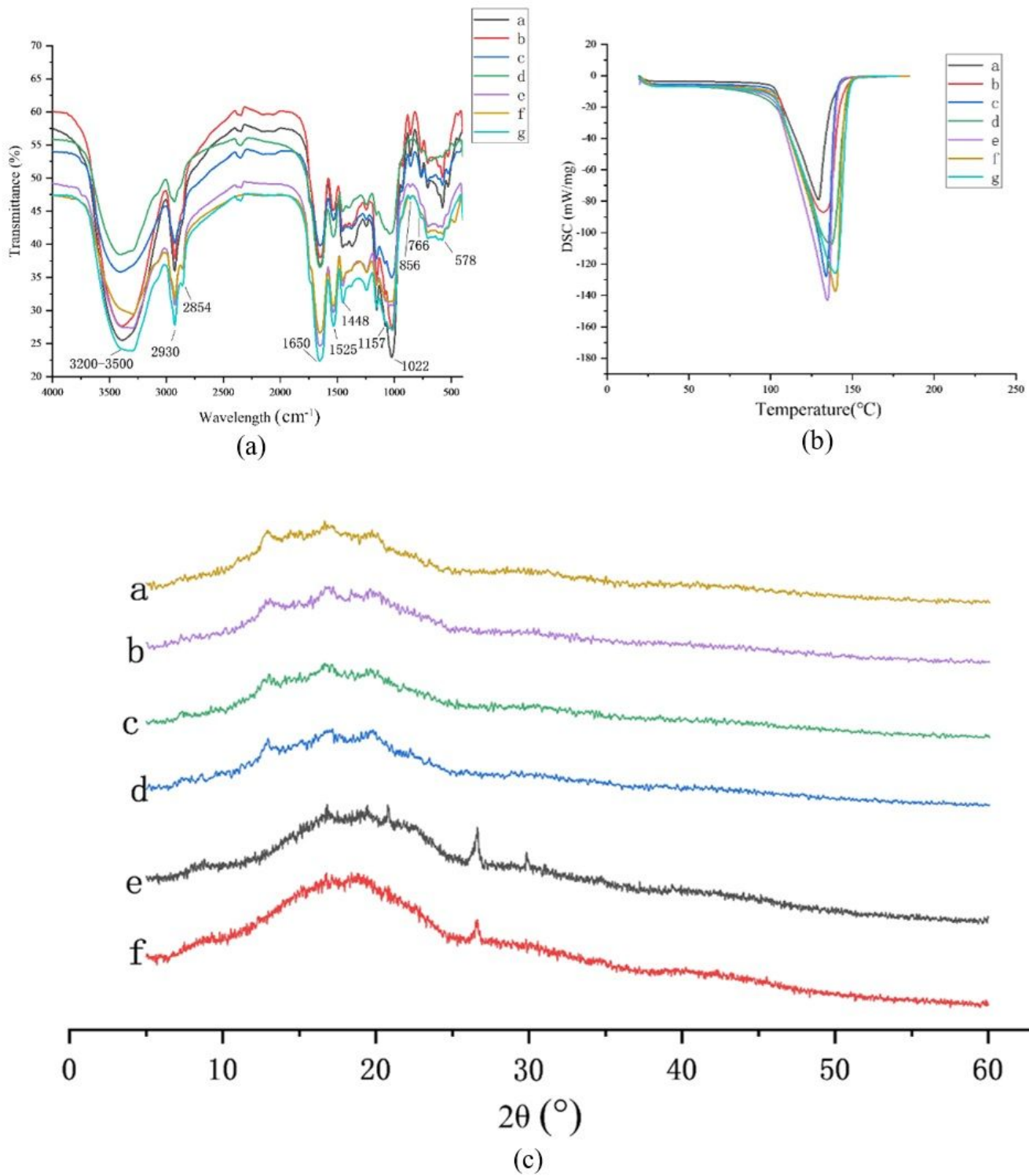


Figure 4

Properties analysis of sorghum starch and distillers' grains starch. (a) FT-IR (b) DSC (c) XRD

Note: a represents the raw sorghum starch; b represents the starch after the first cycle of gelatinization (fermentation day 7); c represents the starch after the second cycle of gelatinization (fermentation day 7); d represents the starch after the third cycle of gelatinization (fermentation day 7); e represents the starch

after the fourth cycle of gelatinization (fermentation day 7); f represents the starch after the fifth cycle of gelatinization (fermentation day 7); g represents the distillers' grains starch

Supplementary Files

This is a list of supplementary files associated with this preprint. Click to download.

- [supplementarymaterial.docx](#)